Transcriptome Analysis of Resistant and Susceptible Mulberry Responses to Meloidogyne Enterolobii Infection

Shao hudie (642928442@qq.com)
Zhongkai University of Agriculture and Engineering https://orcid.org/0000-0001-7115-542X
Yu Fu
Zhongkai University of Agriculture and Engineering
Pan Zhang
Yangtze University
Chunping You
Zhongkai University of Agriculture and Engineering
Chuanren Li
Yangtze University

Research article

Keywords: mulberry, sericulture, Meloidogyne enterolobii, resistance evaluation, transcriptome, resistance mechanism

Posted Date: December 1st, 2020

DOI: https://doi.org/10.21203/rs.3.rs-113699/v1

Version of Record: A version of this preprint was published at BMC Plant Biology on July 16th, 2021. See the published version at https://doi.org/10.1186/s12870-021-03128-w.

Abstract

Background: Mulberry is an important crop for sericulture and root-knot nematode infection is a major factor limiting its production. Understanding the interaction mechanism of mulberry and nematode is important for the control of infection.

Results: Through sequencing and *de novo* transcriptome assembly from root samples of resistant and susceptible mulberry cultivars at different stages after infection with the nematode, *Meloidogyne enterolobii*, we assembled a total of 55,894 unigenes, among which 33,987 were annotated the in Nr, SWISS-PROT, KEGG, and KOG databases. According to GO and pathway enrichment analysis of differentially expressed genes (DEGs), key genes were involved in hormone metabolic processes, plant hormone signal transduction, flavonoid biosynthesis, phenylpropanoid biosynthesis, and peroxisomal and photosynthetic pathways. Analysis of key trends in co-expression networks, indicated that expression of unigenes 0015083, 0073272, 0004006, and 0000628 was positively correlated with resistance to *M. enterolobii*. Unigene 0015083 encodes tabersonine 16-O-methyltransferase, ROMT, which is involved in alkaloid biosynthesis. Unigene 0073272 encodes a transcription factor, which contributes to nitric oxide accumulation during plant immune responses. Unigenes 0004006 and 0000628 encode the ERF and MYB transcription factors, respectively, involved in plant hormone signaling. To verify the accuracy of transcriptome sequencing results, 21 DEGs were selected for RT-qPCR verification; the results confirmed the reliability of the sequencing data.

Conclusions: The results of the present study increase understanding of and provide insights into the resistance mechanisms and candidate genes involved in mulberry-*M. enterolobii* interaction. Thus, our data will contribute to the development of effective control measures against this pathogen.

Background

Mulberry (*Morus alba* L.) is an economically important sericulture crop. Mulberry production can not only be used for sericulture and silk weaving, but also for health care products, medicine, edible fungus cultivation, and other high value-added fields (Qiao, 2012). With the development of the sericulture industry, several pests and diseases have occurred in rapid succession, inducing root-knot nematode disease, which is an important disease of mulberry, occurring in mulberry plantations across China (Tian 2000). Zhang et al. (2020) identified the pathogen causing mulberry root-knot nematode disease in Guangdong Province as *Meloidogyne enterolobii*, using morphological and molecular identification methods. *M. enterolobii* can parasitize a variety of economic crops and tropical fruits and reproduces rapidly. Further, *M. enterolobii* can overcome the resistance response mediated by Mi-resistant nematode genes, parasitize and multiply on resistant tomatoes, peppers and other vegetables. The resulting yield loss can reach more than 65% (Zhuo et al. 2008). And the European and Mediterranean Plant Protection Organization included this species in the EPPO A2 lists in 2010 (Freitas et al. 2014). To date, *M. enterolobii* has been detected in Hainan, Guangdong, Fujian, Hunan, and Yunnan, among other regions of

China (Wang et al. 2015a; Long et al. 2015; Wang et al. 2015b; Huang 2014; Zhuo et al. 2008), with a gradual northward spread noted (Wu et al., 2019).

During the long process of evolution, plants have formed complete basic defense systems in the face of invading root knot nematodes. The first basic line of defense is established by extracellular immune receptors that recognize pathogen associated molecular patterns (PAMP) corresponding to various pathogens (Rehman et al. 2016). The immune response caused by PAMP monitoring is referred to as PAMP-triggered immunity (PTI). Molecules triggering PTI responses, such as Flg22, induce the expression of PTI response-related genes, which causes reactive oxygen species (ROS) bursts, stomata closure, and callose accumulation (Kiba et al. 2020). Nevertheless, pathogens have evolved mechanisms to overcome this first line of plant basic immune defense, and can suppress plant immunity by secreting effectors, which may directly inhibit plant immunity-related proteins or change their active state (Rehman et al. 2016). Hence, various regulation factors work in concert with each other in a highly controlled regulatory network (Bei et al. 2018). Transcriptome sequencing technology can help to reveal the crosstalk and integration pathways between plant (resistance/ susceptible) and nematodes (Bei et al. 2018). Comparative transcriptome analysis using RNA-seq represents an affordable and high-resolution approach to identify differentially expressed genes (DEGs) in response to diverse biotic stresses and has been used in many model and non-model species (Bei et al. 2018). Haegeman et al. (2012) sequenced *Meloidogyne graminicola* on the Illumina 454 sequencing platform, using a *de novo* sequencing approach. Further, Santini et al. (2016) studied the host transcription spectrum during the affinity interaction between *Phaseolus vulgaris* and *Meloidogyne incognita*, and identified 797 host genes as differentially expressed, while Shukla et al. (2018) studied the interaction of susceptible and resistant tomato varieties with *M. incognita* using transcriptome analysis.

RNA-seq has been successfully used to identify nematode-host interactions in several different hosts (Haegeman et al. 2012); however, no study has yet been conducted to understand the nematode-host interaction in mulberry plants. In this investigation we analyzed transcriptome data from disease-resistant and -susceptible varieties of mulberry infected by root-knot nematodes.

Results

Transcriptome sequencing.

Transcriptome sequencing of root samples collected at different time points from two mulberry varieties infected with *M. enterolobii* was carried out on the Illumina platform (Table 2). The proportion of high-quality sequences after filtration of all samples was > 99%, Q20 (%) was > 98%, and Q30 (%) was > 94%, indicating that the transcriptome data were good quality and the sequencing results highly reliable (Table 4).

Table 1
Primer sequences

Unigene ID	Forward primer	Reverse primer
0014355	TCTCCCGTCTCATCGAGGCTTA	ACCAAGCACGTTGGCTCTCTA
0066216	TCTGGCCAAGCAGATCAACGA	ATCTTTCCCCTGAGCTTGACGC
0050791	GTGCTGTTCTTCGACGCTCTCA	TTTCCTCCCGATCCGAACTCCA
0065349	AACGTCGCAAAGGGTTCTCC	TGCCACAAGCCCTATTGCAG
0062337	TTTCGGTTGGCGCGAACATC	AGCAAGCAACGACGGAACCA
0023187	ACCGCCACAGGCTAATGAAGT	TGGTGTCTGTCCCTTGGCTT
0047645	TGGCTGATGTTTGTGGCCTTGA	AGTTGCTCTTTGATTGGTGGTGG
0026072	TTCTGCTGATACGGCGTCCT	TAGGGCCGCAGAGCTTGATT
0002892	GGCATGGCTACTTCCATGTGGT	ATGGTTGGGTTTGCGCTTCC
0008985	AGCTCCATTTGGAACGCGGA	GTCGAATCCCTTGTATGAGGCCA
0059588	GCAGCAGATGATGGCCTTTC	TGGCGCTTCTTCTCCTTGAG
0059369	CGTCAAGGCCAAGACCAATTTCC	CGCCGACGTTGATGTTGTTCTC
0017931	ATTGGAATCCGAAGCCGTGGA	TGTCGCCTTTCCGTCCAATCT
0004573	GCATCTCTAGTGGCTGCTGCTT	TGGCCGTCTTCAGAGGTTGT
0018547	TTTTCCGCCGGGTCGATGTT	TTGACGGCAGTGGCATGAGA
0026157	AGAAGGAGGAGGAAGAGGAAGTGT	TGAGGCACGTTTGCGAAGCA
0070844	AGTTCTTCATCCGTCGCTCCA	ACAATCTCGCAGACGGCACA
0026640	TGATCCAACGAGGGGGTCAT	GGCTTGAATGAAGAAGTTGCTCGG
0014688	AGTGGGCGACCAGATCAACA	TGGTTGAGAGTGCCGGTCTT
0069934	TCGACATTTTCGGGAAGGCCA	AGCATCATCGGAGTCGCTGT
0071495	GCAATGGGGACTGTGACAACA	AGGCATGCCAAAGCTCCAAG
β-actin	AGCAACTGGGATGACATGGAGA	CGACCACTGGCGTAAAGGGA

Table 2
qPCR reaction system

Component name	Add amount
2 × SYBR Green Pro Taq HS Premix	10μL
Primer F (10 μM)	0.4μL
Primer R (10 μM)	0.4μL
Template	2μL
RNase free water	up to 20μL

Table 3
Conditions for qPCR reaction

Reaction stage	Temperature	Time	Cycle
Predenaturation	95℃	30sec	1
Amplification	95℃	5sec	40
	65℃	30sec	
Melting curve	95℃	30sec	1
	65℃	30sec	
	95℃	-	
Condensation	40℃	10sec	-
Note: 1. When setting the annealing temperature of the amplification stage to 65 °C, you need to select Single in the Acquisition Mode (Acquisition Mode), It means that fluorescence signals will be collected during this period.			
2. It is necessary to select Continuous in the acquisition mode of the second 95 °C stage of the melting curve without setting the time.			

Table 4
Transcriptome sequencing data analysis

Sample	Raw reads, n[a]	Clean reads, n (%)[b]	Q20 (99% base call accuracy), %[c]	Q30 (99.9% base call accuracy), %[d]	GC content, %[e]
KB0d-□	60909044	60493992 (99.32%)	98.2	94.71	46.43
KB0d-□	62997456	62491878 (99.2%)	98.68	96.05	45.91
KB0d-□	66197912	65647714 (99.17%)	98.5	95.33	46.73
GB0d-□	54258632	53912710 (99.36%)	98.31	94.91	46.89
GB0d-□	64601656	64131504 (99.27%)	98.78	96.17	46.9
GB0d-□	63892702	63436502 (99.29%)	98.83	96.35	47.0
KBjz8d-□	59244696	58881156 (99.39%)	98.33	94.97	47.05
KBjz8d-□	60152896	59777740 (99.38%)	98.22	94.69	47.23
KBjz8d-□	57259132	56906180 (99.38%)	98.31	94.91	47.33
KBck8d-□	60755908	60391936 (99.4%)	98.32	94.92	47.74
KBck8d-□	52040558	51686572 (99.32%)	98.26	94.81	47.29
KBck8d-□	64174538	63719678 (99.29%)	98.27	94.82	47.34
GBjz8d-□	68430676	67917050 (99.25%)	98.22	94.72	47.96
GBjz8d-□	63719816	63292076 (99.33%)	98.26	94.81	47.32
GBjz8d-□	61292316	60748664 (99.11%)	98.22	94.77	46.92

Notes: [a]Number of original data reads; [b]Number of high-quality sequences after filtering and (percentage of raw reads; [c]Percentage of bases with an accuracy of ≥ 99% after filtering; [d]Percentage of bases with an accuracy of ≥ 99.9% after filtering; [e]Percentage of G/C nucleotides in the sequence.

Sample	Raw reads, n[a]	Clean reads, n (%)[b]	Q20 (99% base call accuracy), %[c]	Q30 (99.9% base call accuracy), %[d]	GC content, %[e]
GBck8d-	48996092	48647074 (99.29%)	98.28	94.88	47.62
GBck8d-	85457146	84877082 (99.32%)	98.29	94.9	48.08
GBck8d-	63423860	62959404 (99.27%)	98.16	94.6	46.78
KBjz17d-	81179024	80436262 (99.09%)	98.2	94.69	47.1
KBjz17d-	64554492	64163368 (99.39%)	98.33	94.93	47.82
KBjz17d-	50325862	50006746 (99.37%)	98.32	94.91	47.69
KBck17d-	57315338	56890984 (99.26%)	98.25	94.83	48.96
KBck17d-	58278390	57858956 (99.28%)	98.32	95.01	49.78
KBck17d-	60404646	59916916 (99.19%)	98.85	96.37	48.53
GBjz17d-	60396566	59987776 (99.32%)	98.4	95.15	47.6
GBjz17d-	73025484	72582168 (99.39%)	98.33	94.98	47.74
GBjz17d-	72193056	71733542 (99.36%)	98.2	94.63	47.68
GBck17d-	54270666	53902126 (99.32%)	98.44	95.29	46.68
GBck17d-	64310188	63735094 (99.11%)	98.72	96.18	46.82
GBck17d-	55197462	54697628 (99.09%)	98.69	96.14	47.8
KBjz23d-	59095200	58691120 (99.32%)	98.31	94.93	47.14

Notes: [a]Number of original data reads; [b]Number of high-quality sequences after filtering and (percentage of raw reads; [c]Percentage of bases with an accuracy of ≥ 99% after filtering; [d]Percentage of bases with an accuracy of ≥ 99.9% after filtering; [e]Percentage of G/C nucleotides in the sequence.

Sample	Raw reads, n[a]	Clean reads, n (%)[b]	Q20 (99% base call accuracy), %[c]	Q30 (99.9% base call accuracy), %[d]	GC content, %[e]
KBjz23d-	79210406	78762440 (99.43%)	98.33	94.96	47.72
KBjz23d-	61962352	61612726 (99.44%)	98.41	95.16	47.66
KBck23d-	57595244	57045606 (99.05%)	98.78	96.32	49.15
KBck23d-	63076062	62601422 (99.25%)	98.77	96.3	47.09
KBck23d-	63769422	63342658 (99.33%)	98.83	96.38	47.32
GBjz23d-	64686018	64110442 (99.11%)	98.24	94.82	47.08
GBjz23d-	69797772	69378514 (99.4%)	98.32	94.94	48.46
GBjz23d-	47339138	47004460 (99.29%)	98.22	94.75	49.18
GBck23d-	52537608	52003500 (98.98%)	98.72	96.21	49.64
GBck23d-	60610656	60072490 (99.11%)	98.65	95.94	47.82
GBck23d-	63395176	62774902 (99.02%)	98.71	96.13	48.32

Notes: [a]Number of original data reads; [b]Number of high-quality sequences after filtering and (percentage of raw reads; [c]Percentage of bases with an accuracy of ≥ 99% after filtering; [d]Percentage of bases with an accuracy of ≥ 99.9% after filtering; [e]Percentage of G/C nucleotides in the sequence.

Results of de novo assembly.

Trinity software was used to assemble the obtained clean reads. After assembly, a total of 55,894 unigenes were obtained, with a length range of 201–22,885 bp (mean, 1202 bp; N50, 1964 bp), and a mean GC content of 41.09%. The assembled transcript length distribution is illustrated in Fig. 1.

Unigene function annotation.

Using BLAST X, the assembled unigenes were compared to the protein databases, Nr, SWISS-PROT, KEGG, and KOG (Evalue < 0.00001), to obtain protein function annotation. A total of 33987 unigenes were annotated, of which 33921 were annotated in the Nr database, accounting for 99.8% of all annotated

genes; 20750 were annotated in the SWISS-PROT database, 61.1% of all annotated genes; 13165 were annotated in the KEGG database, 38.7% of all annotated genes; and 17462 were annotated in the KOG database, accounting for 51.4% of all the annotated genes.

Screening for DEGs.

DEGs in resistant and susceptible varieties at different time points were screened using $P < 0.01$ and FC ≥ 2 as the threshold (Fig. 2A). DEGs in the two cultivars at the three time points were compared using Venn diagrams, demonstrating that 2455, 2267, and 1885 DEGs were produced by the susceptible cultivar at 8, 17 and 23 dpi, respectively, among which 1969, 1657, and 1375 DEGs were unique to each time point (Fig. 2B). In the resistant variety, 2324, 4820, and 3584 DEGs were identified at 8, 17, and 23 dpi, respectively, among which 1612, 3621, and 2450 were unique to each time point (Fig. 2C).

Next, DEGs in resistant and susceptible varieties at 17 dpi, relative to before inoculation, were compared using a Venn diagram of DEGs for gb0d-vs-gbjz17d and kb0d-vs-kbjz17d (representing DEGs at GBjz17d and KBjz17d, respectively, relative to those at GB0d and KB0d). The results showed that 8,678 DEGs were unique to the resistant variety at 17 dpi (Fig. 2D), while 2,340 were unique to the susceptible variety, and 2,330 common to both varieties.

GO enrichment analysis of DEGs.

GO enrichment analysis of DEGs in susceptible mulberry at 17 dpi.

Comparing the 2267 DEGs in the susceptible mulberry cultivar at 17 dpi (GBjz17d) with the GO database (Fig. 3A) indicated that they were enriched for 1129 GO entries. There were 747, 280, and 102 GO items in the three major ontologies of biological process, molecular function, and cell component, respectively. The number of down-regulated genes in each item was significantly higher than that of up-regulated genes. In the biological process ontology, the proportions of genes were higher in the classifications, metabolic process, cellular process, and single-organism process. In the ontology of molecular function, the proportion of genes were higher in the classifications, catalytic activity and protein binding. In the cell component ontology, the proportion of genes was higher in the cell, cell part, membrane, organelle, and membrane part classifications (Fig. 3A).

GO enrichment analysis of DEGs in resistant mulberry at 23 dpi.

Comparing the 3584 DEGs in the resistant mulberry cultivar at 23 dpi (KBjz23d) with the GO database (Fig. 3B) demonstrated that they were enriched in 1309 GO entries, including 898, 292, and 119 GO entries in the three major ontologies of biological process, molecular function, and cell composition, respectively. The number of up-regulated genes in each entry was significantly higher than that of down-regulated genes. In the three ontologies, the GO classifications of enriched DEGs for KBjz23d were the same as those for GBjz17d; however, the enriched GO entries differed from those for GBjz17d; in the biological process ontology, KBjz23d DEGs were significantly enriched for entries related to the regulation of

macromolecular metabolism, while GBjz17d DEGs were significantly enriched for entries related to plant cell wall metabolism.

GO enrichment analysis of DEGs between resistant and susceptible varieties.

Comparing samples from resistant and susceptible varieties at 17 dpi, there were 2340 unique DEGs (referred to as KBvsGB-GBjz17d DEGs) in susceptible varieties. Comparison of these DEGs with the GO database showed they were mainly enriched for 1146 GO items (Fig. 4A), including 776, 258, and 112 in the ontologies biological process, molecular function, and cell composition, respectively. The number of down-regulated genes was significantly higher than that of up-regulated genes. In the biological process ontology, the proportion of genes was higher in the classifications metabolic process, cellular process, and single organization process, while for the molecular function ontology, the proportion of genes was higher in the classifications catalytic activity and protein binding, and in the cell component ontology, the percentage of genes in the classification cells and cell parts was higher (Fig. 4A).

Next, the 8678 unique DEGs in resistant varieties (KBvsGB-KBjz17d DEGs) were compared with the GO database. The results suggested (Fig. 4B) that KBvsGB-KBjz17d DEGs were mainly enriched in 1764 GO entries, among which there were 1179, 422, and 163 GO entries in the three major ontologies, biological process, molecular function, and cell composition, respectively. The number of down-regulated genes in each entry was significantly higher than that of up-regulated genes. In the three ontologies, the GO classifications enriched for KBvsGB-KBjz17d DEGs was the same as that of KBvsGB-GBjz17d (Fig. 4), while the enriched GO entries differed from those of KBvsGB-GBjz17d. In the cell component ontology, KBvsGB-KBjz17d DEGs were significantly enriched for items including ribosomes and cell-matrix (Fig. 4C), while those of KBvsGB-GBjz17d were significantly enriched for items related to photosynthesis, such as thylakoid membranes (Fig. 4D).

Pathway enrichment analysis of DEGs.

Pathway analysis is helpful for understanding gene biological functions, and for identifying key signal transduction and biochemical metabolism pathways involving DEGs.

Pathway enrichment analysis of DEGs in susceptible mulberry at 17 dpi.

Pathway annotation of DEGs in susceptible mulberry at 17 dpi (GBjz17d) using the KEGG database showed that they were enriched in 113 pathways, with five significantly enriched pathways ($Q \leq 0.05$) (Fig. 5A), as follows: biosynthesis of secondary metabolites, ubiquinone and other terpenoid-quinone biosynthesis, flavonoid biosynthesis, phenylpropanoid biosynthesis, and metabolic pathways. Among them, the pathway including the highest number of enriched genes, was the metabolic pathway, which included 145 DEGs. The enrichment factor (rich factor) value of the flavonoid synthesis pathway was the highest, indicating that the pathway was the most enriched.

Pathway enrichment analysis of DEGs in resistant mulberry at 23 dpi.

DEGs from resistant mulberry at 23 dpi (KBjz23d) were annotated with pathways using the KEGG database. The results showed that DEGs were enriched in 109 pathways, six of which were significantly enriched ($Q \leq 0.05$) (Fig. 5B): biosynthesis of secondary metabolites; glucosinolate biosynthesis; cutin, suberine, and wax biosynthesis; alpha-linolenic acid metabolism; phenylpropanoid biosynthesis; and flavonoid biosynthesis. Among these, the pathway enriched for the most genes was secondary metabolite synthesis, including 107 DEGs. The glucosinolate synthesis and cutin, suberine, and wax biosynthesis pathways showed the highest level of enrichment.

Pathway enrichment analysis of DEGs between resistant and susceptible varieties.

DEGs with expression differences between resistant mulberry before inoculation and susceptible mulberry at 17 dpi (KBvsGB-GBjz17d) were annotated for pathway enrichment using the KEGG database, demonstrating that DEGs were enriched for 111 pathways, of which two were significantly enriched ($Q \leq 0.05$) (Fig. 6A): ubiquinone and other terpenoid-quinone biosynthesis and cutin, suberine and wax biosynthesis. Cutin, suberine and wax biosynthesis was the most strongly enriched.

Annotation of DEGs with expression differences between resistant mulberry before inoculation and at 17 dpi (KBvsGB-KBjz17d) by KEGG database analysis showed that they were enriched for 126 pathways, with seven significantly enriched pathways ($Q \leq 0.05$) (Fig. 6B), as follows: starch and sucrose metabolism; pentose and glucuronate conversion interconversions; ABC transporters; phenylpropanoid biosynthesis; plant-pathogen interaction; arginine and proline metabolism; and cyanoamino acid metabolism. Among these pathways' ABC transporters was the most enriched.

DEG expression trends.

The expression trends of DEGs between susceptible mulberry at 17 dpi (GBjz17d), resistant mulberry at 23 dpi (KBjz23d), resistant mulberry before inoculation and susceptible mulberry at 17 dpi (KBvsGB-GBjz17d), and resistant mulberry before inoculation and susceptible mulberry at 17 dpi (KBvsGB-KBjz17d) were analyzed, resulting in identification of 20 trends. In the trend graphs, colors indicate significantly enriched trends, while those without color are non-significantly enriched trend blocks (Fig. 8–12).

GBjz17d DEG expression trends.

Trend analysis of GBjz17d DEGs identified profile2, profile1, profile18, profile16, profile17, and profile3 (Fig. 7A) as significantly enriched trends, including 452, 312, 210, 219, 196, and 169 genes, respectively (Fig. 7B).

KBjz23d DEG expression trends.

Trend analysis of KBjz23d DEGs identified profile17, profile2, profile19, profile0, profile12, and profile15 (Fig. 8A) as significantly enriched trends, including 627, 260, 349, 333, 260, and 342 genes, respectively (Fig. 8B).

Expression trends of DEGs between resistant and susceptible varieties.

Trend analysis KBvsGB-GBjz17d DEGs (Fig. 9A) revealed profile2, profile17, profile1, profile16, profile18, profile7, and profile0 as significantly enriched and including 461, 347, 244, 307, 227, 136, and 106 genes, respectively (Fig. 9B).

Trend analysis of KBvsGB-KBjz17d DEGs (Fig. 10A) showed that profile2, profile1, profile17, profile18, profile12, profile3, profile7, and profile0 were enriched, including 2003, 953, 1373, 492, 346, 423, 294, and 306 genes, respectively (Fig. 10B).

Co-expression network analysis of key trends.

The core gene, with the highest connectivity in GBjz17d profile1, was unigene 0015188; the co-expression network diagram for this gene is presented in Fig. 11A. Unigene 0015188 encodes β-galactosidase, which is involved in the degradation of pectin in plant primary cell walls. The core gene with the highest connectivity in GBjz17d profile3 was unigene 0022838, and the related co-expression network is presented in Fig. 11B. Unigene 0022838 encodes CASP like protein 1C1, which is related to plant stress resistance. Core genes with high connectivity in the GBjz17dprofile16 were unigenes 0022247 and 0010321; the related co-expression network is shown in Fig. 11C. Unigene 0022247 encodes 3-hydroxy-3-methylglutaryl coenzyme A reductase, which is a key enzyme for antitoxin and steroid based synthesis of sesquiterpenoids, while unigene 0010321 may encode a leucine rich repeat receptor protein kinase (LRR-RLK), which is involved in plant hormone signal transduction, recognition, and transmission between plants and pathogens. The core gene with high connectivity in GBjz17d profile18 was unigene 0021656, and the related co-expression network is detailed in Fig. 11D. Unigene 0021656 encodes calmodulin dependent protein kinase type I, and KEGG annotation showed that this gene is part of the plant-pathogen interaction pathway.

The core gene with highest connectivity in kbjz23d profile0 was unigene 0014848; the related co-expression network diagram is shown in Fig. 11E. Unigene 0014848 encodes ubiquitin carboxy terminal hydrolase 12, which is an effector protein that can inhibit the resistance of plants to root-knot nematodes and promote the formation of nematode feeding points. In kbjz23d profile12, the core gene with highest connectivity was unigene 0015083; the related co-expression network is shown in Fig. 11F. Unigene 0015083 encodes a 16-o-methyltransferase ROMT protein involved in plant alkaloid synthesis. The core genes with higher connectivity in the kbjz23d profile15 were unigenes 0073558 and 0073272, and the related co-expression network is shown in Fig. 11G. Unigene 0073558 encodes ubiquitin carboxyl terminal hydrolase 13, while unigene 0073272 encodes the srg1 protein, which belongs to the zinc finger transcription factor family. The expression of srg1 is related to the accumulation of nitric oxide during plant immune responses. Further, GO biological process annotation showed that this gene is related to flavonoid synthesis. The core genes with higher connectivity in kbjz23d profile19 were unigenes 0002889 and 0068389, the related co-expression network diagram is shown in Fig. 11H. Unigene 0002889 encodes protein phosphatase 2C, which can regulate abscisic acid (ABA) signal transduction and unigene

00683889 encodes a protein kinase. Cipk14, which plays a role in stress responses; GO biological annotation indicated that this gene is related to cell process regulation.

The core gene with higher connectivity in kbvsgb-kbjz17 dprofile3 was unigene 0004006, and the related co-expression network is shown in Fig. 11I. Unigene 0004006 encodes an ERF transcription factor, which is involved in signal transmission using salicylic acid (SA), ethylene, jasmonic acid (JA), and other factors, and plays an important role in plant stress response. In kbvsgb-kbjz17dp profile12, core genes with higher connectivity were unigenes 0000628 and 0015083, and the related co-expression network diagram is presented in Fig. 11J. Unigene 0000628 encodes the MYB transcription factor family protein, AIM1, which contributes to stress-related gene expression during ABA signal transmission and positively regulates plant defense responses to pathogens. Unigene 0015083 encodes a rumt glycyrrhizin-16-o-methyltransferase gene, associated with plant alkaloid synthesis. The core genes with higher connectivity in kbvsgb-gbjz17d profile16 were unigenes 0052595 and 0004809, and the related co-expression network is shown in Fig. 11K. Unigene 0052595 encodes the autophagy-related factor, Atg8, which is under threat in plants. Unigene 0004809 encodes cell wall-related receptor kinase 22, which belongs to the RLK receptor kinase family involved in plant defense.

RT-qPCR validation of DEGs.

To verify the accuracy of the transcriptome sequencing results, 21 DEGs were analyzed by RT-qPCR using cDNA obtained by reverse transcription of the RNA used for sequencing as the template. Relative gene expression levels were calculated using the $2^{-\Delta\Delta Ct}$ method and GraphPad Prism 8.0 used to visualize the results (Fig. 12). Although the magnitude of differences in expression detected by RT-qPCR were not identical to those of DEGs detected by transcriptome sequencing, the direction of the change of DEG expression was consistent between the two approaches, indicating that the results of transcriptome sequencing were highly reliable.

Discussion

M. enterolobii has been reported as a mulberry root-knot pathogen (Chen et al. 2016). This species has strong virulence and rapid reproduction; thus, it has a high impact on mulberry production. Cultivation of mulberry varieties resistant to *M. enterolobii* is one of the most effective control methods (Shao, 2019); however, the mechanism underlying resistance of mulberry to *M. enterolobii* is not clear. In this study, transcriptome sequencing technology was applied for the first time to study *M. enterolobii* infection of mulberry, with the aim of understanding the interactions between resistant and susceptible mulberry varieties and *M. enterolobii.* In addition, we explored the molecular mechanisms underlying resistance to *M. enterolobii*, thus providing a theoretical knowledge base for breeding resistance mulberry varieties.

At each time point after inoculation of root-knot nematode, the number of down-regulated genes was greater than that of up-regulated genes in susceptible varieties, with the number of DEGs highest at 8 dpi. Our results indicate that the primary plant defense response gradually stabilized in the mid and late

stages of infection (17 and 23 dpi), leading to a decrease in DEGs (Fig. 3). The number of DEGs produced by the resistant variety at 8, 17, and 23 dpi with root nematode first increased and then decreased slightly, with the number of up-regulated genes higher than that of down-regulated genes. These results indicate that the primary defense response of disease-resistant varieties was triggered during the early stage of infection (8 dpi), while with longer infection of the root-knot nematode, the plant produced a more advanced defense system, with induction of numerous defense-related genes, which could explain the observed large increase in the number of DEGs in mid and late infection (17 and 23 dpi). DEGs between resistant and susceptible mulberry varieties infected with *M. enterolobii* in this study were consistent with those of resistant and susceptible watermelon materials infected with *M. incognita*, as reported by Zhao (2018). The bioinformatics analysis of these DEGs showed that the related processes involved in nematode resistance include active oxygen removal, cellulose, lignin, diabetic synthesis, and ABA signaling. In these processes, the expression of many key genes is positively correlated with resistance to Meloidogyne incognita

GO and pathway enrichment analysis of DEGs at 17dpi and 23dpi were performed for resistant and susceptible varieties. Four different gene sets were enriched in the same GO classification, and the enriched pathways also contained secondary metabolite synthesis pathways related to plant disease resistance, such as phenylpropane synthesis, flavonoid synthesis, and quinone synthesis. These data show that both resistant and susceptible mulberry varieties deploy similar defense processes after infection. GO enrichment analysis indicated that the number of down-regulated genes in this GO classification in susceptible varieties was higher than the number of up-regulated genes, while the opposite was the case (i.e. number of up-regulated genes was greater than the number of down-regulated genes) in the disease-resistant variety. Further, the number of DEGs from resistant varieties annotated in the GO database was much higher than that in susceptible varieties. This is consistent with results reported by Xing (2016), and shows that resistant varieties can initiate expression of a large number of defense-related genes following infection to improve their resistance to pathogens.

Phenylpropane is a low molecular weight antibiotic, insect repellent, or signaling molecule involved in interactions between plants and microbes, by participating in plant defense responses (Ohri and Pannu 2010). The synthesis of phenylpropanes is related to the production of disease-resistant secondary biomass, including plant protection factors, lignin, and phenolic compounds, which is a potential method of improving plant resistance to nematodes (Yu and Tang 1999). Wuyts et al. (2007) studied the lignin and phenylpropane content in the roots of resistant and susceptible bananas and infected by *Radopholus similis* and found that lignin and ferulic acid (phenylpropane) content were higher in the vascular bundle of resistant varieties than that in susceptible varieties; all types of vascular bundle exhibited lignification induced by infection. Xu et al. (2008a) showed that, after infection with *M. incognita*, phenylpropanes content and related enzyme activities in the roots of resistant eggplant were greater than those susceptible varieties. In the present study, genes related to phenylpropane synthesis in susceptible mulberry began to down-regulate at 17 dpi with nematodes, while the resistant variety showed up-regulated expression. This may be one of the reasons for the differences in resistance between resistant and susceptible varieties.

Quinone and flavonoid are phenolic compounds that function as secondary metabolites (Hua,2017). Phenolic compounds are established as important in interactions between plants and pathogens (ref). Dama (2002) measured the activity of three types of quinone extracted from plants in killing *Meloidogyne javanica*. The results suggested that the three substances tested had different degrees of nematode killing activity, with the killing rate of baihuadan-quinone reaching 100%. Hutangura et al. (1999) reported that the formation of giant cells in *Trifolium repens* was related to auxin accumulation, and flavonoids can act as auxin transport regulators, potentially controlling auxin accumulation. Further, flavonoids can inhibit *M. incognita* activity (Wuyts et al. 2006) and flavonoid production is a plant defense response to nematode infection (Furlanetto et al. 2007). Wasson et al. (2009) demonstrated that flavonoids can influence the size and cell division of root-knots, while they are not involved in root-knot formation or mega cell formation and it is unlikely that auxin transport and accumulation are mediated by the root-knot. In this study, we found that genes related to phenolic compound synthesis were down-regulated in susceptible mulberry plants in the later stages of infection, while they were up-regulated in resistant varieties.

Infection with root-knot nematodes can influence plant photosynthesis, which is a basic physiological activity of plants, required for producing organic matter and storing energy. Loveys and Bird (1973) observed that the rate of photosynthesis decreased significantly in the early stage of infection by *M. javanica* compared with controls. Further, Ye et al. (2011) studied the effects of nematode infection on the photosynthesis of resistant and susceptible greenhouse-grown cucumber leaves and showed that chlorophyll content and net photosynthetic rate of both resistant and susceptible materials decreased after infection; however, these decreases were significantly smaller in resistant materials than the susceptible materials. Zhao (2018) also found that the expression of genes related to photosynthesis, chlorophyll-binding, the photosynthetic system, and other processes were inhibited in the early stage of *M. incognita* infection of resistant and susceptible watermelon varieties, using transcriptome sequencing technology. In this study, genes related to resistance, photosynthesis, and the thylakoid were inhibited in the early stage of nematode infection, consistent with previous findings.

Zeatin synthesis and enrichment of peroxidase-related genes were detected in susceptible mulberries. Zeatin is a cytokinin (Shen, 2000), and levels of cytokinins are altered when plants are under stress (Angra-Sharma and Sharma, 2000). Lohar et al. (2004) showed that the expression of cytokinin response regulatory genes decreased when root-knots developed in plant roots, and the overexpression of cytokinin oxidase in *Lotus japonicus* can reduce the number of nematode-infected root-knots. In this study, the inhibition of zeatin synthesis in infected susceptible mulberry varieties may be related to the production of giant cells. Peroxidase is an important plant protective enzyme, which is related stress resistance (Hu, 2015). Xu et al. (2008b) proposed that the low peroxidase activity of resistant eggplants infected by root-knot nematodes is beneficial to the accumulation of reactive oxygen species and facilitates allergic necrosis in plant roots. Jin et al. (2009) observed the tendency of peroxidase activity to first increase and then decrease in the early stage (0–25 days) of *M. incognita* infection of black seed pumpkin. In this study, the expression of peroxidase-related genes was first up-regulated and then down-regulated after infection of susceptible mulberry. Damage of the root cell membrane of susceptible mulberry cultivars in

the early stage of nematode infection, may accelerate enzymatic reactions; therefore, related genes exhibit up-regulated expression, and changes in root cells tended to be relatively slow in the later stages of infection, and related genes began to be down-regulated.

In the resistant mulberry variety, genes related to SA metabolism and terpene synthesis were also enriched, and showed up-regulated expression. SA is a simple phenolic compound involved in signal transduction and can induce expression of pathogenicity-related proteins and plant systemic acquired resistance (Malamy et al. 1990). Further, it is an important signaling molecule causing plant allergic reactions to root-knot nematodes (Branch et al. 2004). Terpenes are important secondary metabolites in plants, which function in regulating plant growth and development, resisting photooxidative stress, and directly or indirectly participate in plant defense (Yue and Fan 2011). Echeverrigaray et al. (2010) studied the nematode activity of 22 monoterpene compounds, demonstrating that 20 of them could significantly reduce the hatching rate of nematode eggs, while 11 could reduce the mobility of root-knot nematodes. In this study, SA metabolism and the terpenoid pathway were only enriched in the disease-resistant mulberry variety, indicating that, compared with the susceptible mulberry variety, the resistant mulberry employs different defense mechanisms following infection.

In addition to the enrichment of genes related to SA metabolism and terpenoid synthesis, some core genes with high connectivity were zinc-finger, MYB, and ERF transcription factors involved in the resistant mulberry variety co-expression network. Transcription factors can improve plant resistance by regulating signal transduction involved in plant immune responses in response to attack by biological and non-biological factors. In this study, the core gene, unigene 0073272, encodes the zinc finger transcription factor, srg1, whose expression is positively regulated by nitric oxide in plants and can activate plant defense responses (Cui et al. 2018). Ali et al. (2013) found that overexpression of the ERF transcription factor, RAP2.6, in *Arabidopsis thaliana* led to increased expression of JA-responsive genes after *Heterodera schachtii* infection, resulting in increased callose deposition in syncytia and increased *A. thaliana* resistance to *H. schachtii*. Abuqamar et al. (2009) reported that decreased expression of slaim1 in *Solanum lycopersicum* increased the susceptibility of tomato plants to *Botrytis cinerea*, and that slaim1 is sensitive to salt stress, and Abuqamar et al. (2009) suggested that the gene may respond to pathogen and abiotic stress by promoting ABA signal transmission in tomato.

There are few studies on transcription factors encoding genes related to disease resistance in mulberry and analysis of these genes in follow-up studies will assist in future mulberry resistance breeding. By screening for DEGs during the infection process and determining the molecular mechanisms underlying mulberry resistance to root-knot nematode disease, our data provide a theoretical basis for cultivation of disease-resistant mulberry varieties. In addition, the detailed transcriptome data generated in this study may facilitate the identification of genes that can be targeted to increase the resistance of mulberry to *M. enterolobii.*

Conclusions

In this study, transcriptome sequencing and Denovo assembly were used to construct reference transcripts of resistant and susceptible mulberry varieties which infected by *M. enterolobii*. Through the selection and enrichment analysis of DEGs, trend analysis of DEGs and co-expression network analysis of DEGs, it revealed the gene expression of resistant and susceptible mulberry after infection. The results of this study show that there are several reasons for the difference in resistance of the resistant and susceptible mulberry species to *M. enterolobii.*The synthesis of secondary metabolites related to plant disease resistance in resistant varieties continued to be up-regulated, while the synthesis of secondary metabolites related to plant disease resistance in susceptible varieties was inhibited. Transcription factor-related genes in resistant varieties are highly connected and up-regulated. In susceptible varieties, the signal recognition and transmission of plants to *M. enterolobii* and the down-regulated expression of genes related to plant defense.

Methods

Nematode culture.

M. enterolobii eggs were isolated from the roots of mulberry plants in the sericulture teaching base at South China Agricultural University and used for inoculation, as described below.

Plant growth conditions.

The experimental cultivar, Yuesang C44, is resistant to *M. enterolobii*, while 283 × anti-10 is a susceptible cultivar (Shao et al. 2019). Germination induction and transplantation were conducted following the method described in Wu (2009).

Nematode collection and inoculation.

Nematode collection was according to the method of Li et al. (2016). Inoculation was conducted using 60-day-old mulberry seedlings grown under greenhouse conditions. First, the soil above the roots of the plant was removed to expose the root system. Then, 2 mL of egg suspension was added into the soil near the roots using a pipette. After inoculation, roots were covered with soil. Control group plants were inoculated using 2 mL of water. Fifteen pots were inoculated for each treatment. Mulberry seedlings were placed in a greenhouse and watered regularly.

Collection of mulberry seedling root samples.

Based on preliminary experiments, when 500 nematode eggs were inoculated, susceptible mulberry varieties began to produce root knots at 17 days post-inoculation (dpi) after inoculation, while resistant varieties start to produce root knots at 23 dpi. Therefore, in this experiment samples were collected at four time points, as follows: on inoculation (day 0), and 8, 17, and 23 dpi. At each time point, 10 samples were taken from each experimental group, including control groups, of each of the two varieties, and samples pooled in groups of three or four, to generate three samples for each inoculated and control variant at each time point. Samples of resistant varieties at each time point were numbered as follows: before

inoculation, KB0d; and at 8 dpi, KBjz8d and KBck8d; 17 dpi, KBjz17d and KBck17d; and 23 dpi KBjz23d, KBck23d, where samples including the letters ‘jz’ were inoculated with nematode and those with ‘ck’ were water inoculated controls. Similarly, samples of susceptible varieties were numbered GB0d, GBjz8d, GBck8d, GBjz17d, GBck17d, GBjz23d, GBck23d. Technical replicates (samples collected at the same time points from the same experimental groups) were numbered □, □, and □, giving 42 samples in total. Root-knot samples were collected according to the method described by Li (2016).

Transcriptome sequencing and data analysis.

Samples were sent to Guangzhou Jidio Biotechnology Co., Ltd. for RNA extraction and transcriptome sequencing on the Illumina Hiseq 4000 platform using the PE150 double-ended sequencing approach. Since there is no complete reference genome information for mulberry in NCBI GenBank, Trinity software was used for *de novo* genome assembly, based on the sequencing results, according to the non-reference genome, mulberry reference transcripts were obtained, and unigene functional annotation and differential expression analysis conducted on the resulting sequence assembly, followed by GO function enrichment, pathway function enrichment, and trend analyses of selected DEGs were conducted.

Since the susceptible varieties began to develop root knots at 17 dpi and the resistant varieties start to form root knots at 23 dpi, data analysis focused primarily on these two time points (i.e., 17 and 23 dpi) and on DEGs from infected mulberries of the susceptible variety at 17 dpi (GBjz17d) and resistant variety at 23 dpi (KBjz23d). When comparing the changes in resistant and susceptible varieties after infection, GBjz17d and KBjz17d were compared, and the identified DEGs analyzed.

Quantitative analysis of genes and screening for DEGs.

The reads per kilobase per million reads method (Mortazavi et al. 2008) was used to measure the expression of unigenes. DEGs were screened using DESeq2, with $p < 0.01$ and fold-change (FC) ≥ 2 selected as the threshold for significantly differential expression. The experiment comprised one resistant and one susceptible variety, and four-time points for the test and control group samples. Therefore, when analyzing DEGs in resistant and sensitive varieties at different time points after inoculation, those with expression changes due to *M. enterolobii* infection were screened, and DEGs produced by expression changes during natural mulberry growth excluded.

GO terms and KEGG pathways analysis.

DEGs were analyzed using GO (Ashburner et al. 2000) and KEGG pathway enrichment (Nakaya et al. 2013) methods in DAVID (Huang et al. 2008), using the parameters, $p < 0.05$, gene number ≥ 2, and false discovery rate < 0.01.

Series test of cluster of DEGs.

Series Test of Cluster uses STEM software and log2 standardization to preprocess data. The most representative 20 modules are generated by default, and those with $p < 0.05$ considered significantly

enriched trends. After enriched trends were identified, GO and pathway enrichment analysis were carried out for the identified genes in each trend, and GO items and metabolic pathways that were significantly enriched obtained.

Gene co-expression network analysis.

Co-expression network analysis of DEGs included in enrichment trends was conducted. Correlation of all genes in the trend in samples at each time point was evaluated using the Pearson correlation coefficient, and a network diagram drawn based on relationships with Spearman correlation coefficients > 0.9 (Zhao, 2018). The soft threshold was used to calculate gene connectivity, genes arranged according to their level of connectivity, and core genes in the co-expression network (hub genes) selected as those with the highest connectivity.

Validation of DEGs by quantitative real-time PCR (qRT-PCR).

In this study, 21 DEGs related to the infection of *M. enterolobii* were selected for RT-qPCR verification.

Primer design.

The primer design tool in NCBI was used to design RT-qPCR primers (https://www.ncbi.nlm.nih.gov/). Primers (17–25 nucleotides; GC content, 45–55%) were designed to generate PCR products of 80–150 bp, the melting temperatures of the two primers was close to one another, and GC or AT enrichment at the 3' terminus avoided. Following Zhou (2017), we use the β-actin gene (GenBank Accession No.: DQ785808), which is stably expressed in mulberry, as a reference. Primer sequences are provided in Table 1. Primer synthesis was carried out by Tianyi Huiyuan Company (Guangzhou, China).

Reverse transcription of RNA samples.

Reverse transcription (RT) was performed on all RNA samples using Evo M-MLV RT Premix for qPCR (AG11706) from Aikerui Biological Engineering Co., Ltd. (Hunan, China) to synthesize cDNA.

Fluorescence quantitative PCR.

Experiments were performed on a LightCycler® 480 (Roche) fluorescent quantitative PCR instrument using the SYBR® Green Pro Taq HS qPCR Kit from Ecory Bioengineering Co., Ltd (Hunan, China). Prepare the qRCR reaction solution.

 The reaction solution system is shown in Table 2. When configuring, add other reagents except the cDNA template to the 1.5 mL centrifuge tube, mix it, and then aliquot it into the eight-tube tube dedicated for fluorescence quantification. After the aliquot, add the corresponding cDNA to the eight-tube tube. Repeat 3 times, set 3 negative controls for each pair of primers (without cDNA template).

Refer to Table 3 for fluorescence quantitative reaction conditions and reaction.

Abbreviations

DEGs
differentially expressed genes; ROS:reactive oxygen species; EPPO:European and Mediterranean Plant Protection Organization; PAMP:pathogen associated molecular patterns; ABA:abscisic acid; SA:salicylic acid; JA:jasmonic acid; Dpi:days post-inoculation; RT:Reverse transcription

Declarations

Ethics approval and consent to participate

Not applicable.

Consent for publication

Not applicable.

Availability of data and materials

The assembled gene sequences of *M. enterolobii* are available in NCBI. The authors affirm that all data necessary for confirming the conclusions of the article are present within the article, figures, and tables.

Competing interests

The authors declare that they have no competing interests.

Funding

The support for the project: Guangdong modern agricultural industry technology system innovation team project (2016LM1134)

Authors' Contributions

HS operates all relevant experiments, and was a major contributor in writing the manuscript. YF analyzes relevant data of the full text. PZ collect samples. CY guides the operation of the experiment. CL teaches essay writing. All authors read and approved the final manuscript.

The author would like to acknowledge all the teachers and students from the laboratory of the Agricultural College of Zhongkai Agricultural Engineering College for their help. We thank Charlesworth Author Services (https://www.cwauthors.com/) for its linguistic assistance during the preparation of this manuscript.

References

1. AbuQamar S, Luo H, Laluk K, et al. 2009. Crosstalk between biotic and abiotic stress responses in tomato is mediated by the *AIM1* transcription factor. Plant J. 58(2):347-360.
2. Ali M A, Abbas A, Kreil D P, et al. 2013. Overexpression of the transcription factor RAP2. 6 leads to enhanced callose deposition in syncytia and enhanced resistance against the beet cyst nematode *Heterodera schachtii* in Arabidopsis roots. BMC Plant Biol. 13(1):47-55.
3. Angra-Sharma R, Sharma D K. 2000. Cytokinins in pathogenesis and disease resistance of *Pyrenophora teres*-barley and *Dreschslera maydis*-maize interactions during early stages of infection. Mycopathologia 148(2):87-95.
4. Ashburner M, Ball C A, Blake J A, et al. Gene ontology: tool for the unification of biology. The Gene Ontology Consortium[J]. Nature Genetics, 2000, 25(1):25-29.
5. Bei W, Xue-Qi L, Ling H, et al. Whole-transcriptome sequence analysis of *Verbena bonariensis* in response to drought stress. Int. J. Mol. Sci. 2018,19(6):1751-1759.
6. Branch C, Hwang C F, Navarre, D. A., et al. 2004. Salicylic acid is part of the *Mi-1*-mediated defense response to root-knot nematode in tomato. Mol. Plant-Microbe Interact. 17(4):351-356.
7. Chen H, Wang H F, Chen M C. Research progress on root-knot nematode in Elephantia occidentalis[J]. Guizhou Agricultural Sciences, 2016, 44(005):51-55.
8. Cui B, Pan Q, Clarke D, et al. 2018. S-nitrosylation of the zinc finger protein SRG1 regulates plant immunity. Nat. Comm. 9(1):1-12.
9. Dama L B. 2002. Effect of naturally occurring napthoquinones on root-knot nematode *Meloidogyne javanica*. Indian Phytopathol. 55(1):67-69.
10. Echeverrigaray S, Zacaria J, Beltrão R. 2010. Nematicidal activity of monoterpenoids against the root-knot nematode *Meloidogyne incognita*. Phytopathology 100(2):199-203.
11. Freitas V M, Correa V R, Motta F C, et al. 2014. Resistant accessions of wild *Psidium* spp. to *Meloidogyne enterolobii* and histological characterization of resistance. Plant Pathol. 63(4):738-746.
12. Furlanetto C, Phillips M, Jones J. 2007. The role of flavonoids produced in response to cyst nematode infection of *Arabidopsis thaliana*. Nematology 9(5):671-677.
13. Haegeman A, Mantelin S, Jones J T, et al. 2013. Functional roles of effectors of plant-parasitic nematodes. Gene 492(2):19-31.
14. Hu X W, Yao Y L, Xing S L, et al. cDNA cloning and functional analysis of SsPOD-1 gene (SsPOD-1) [J]. Chinese Journal of Tropical Crops, 2015, 36(007):1290-1296.

Figures

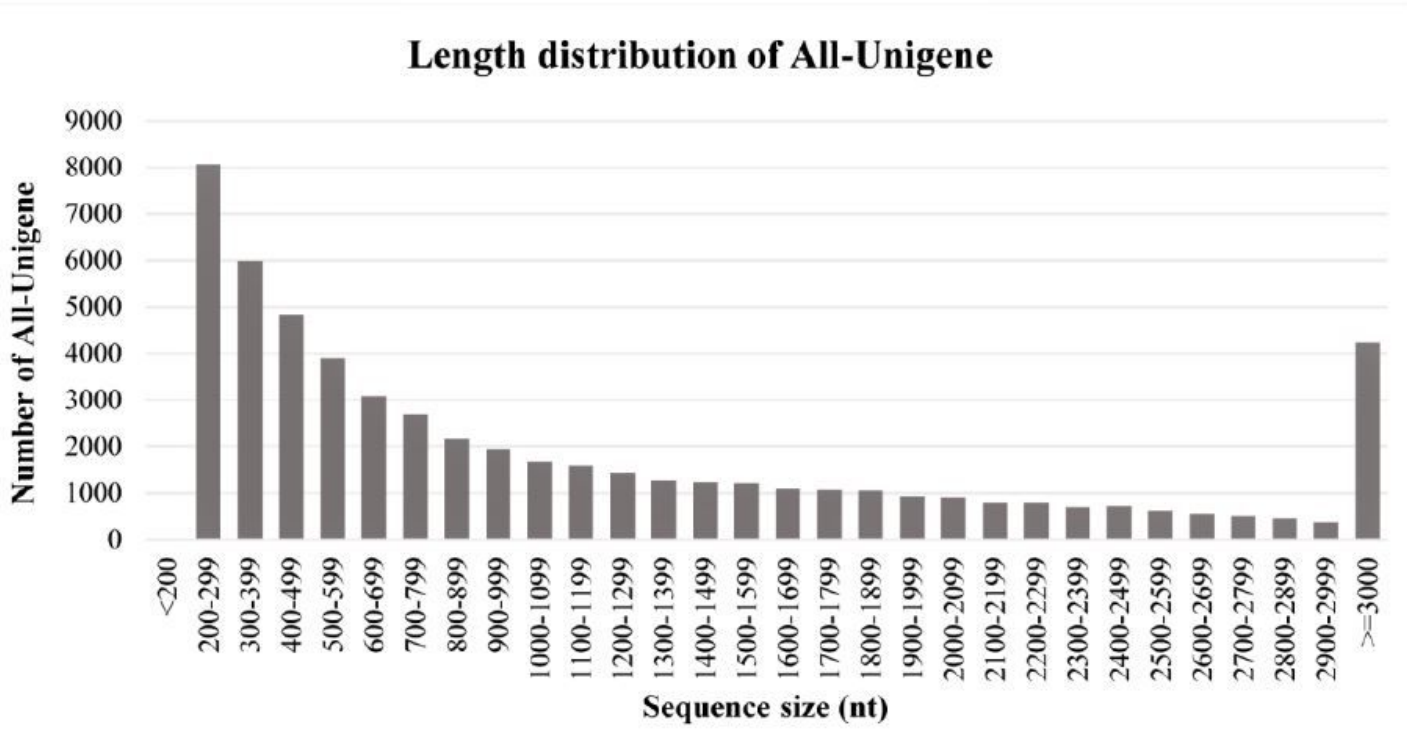

Figure 1

Fig. 1 The length of distribution statistics of the transcript

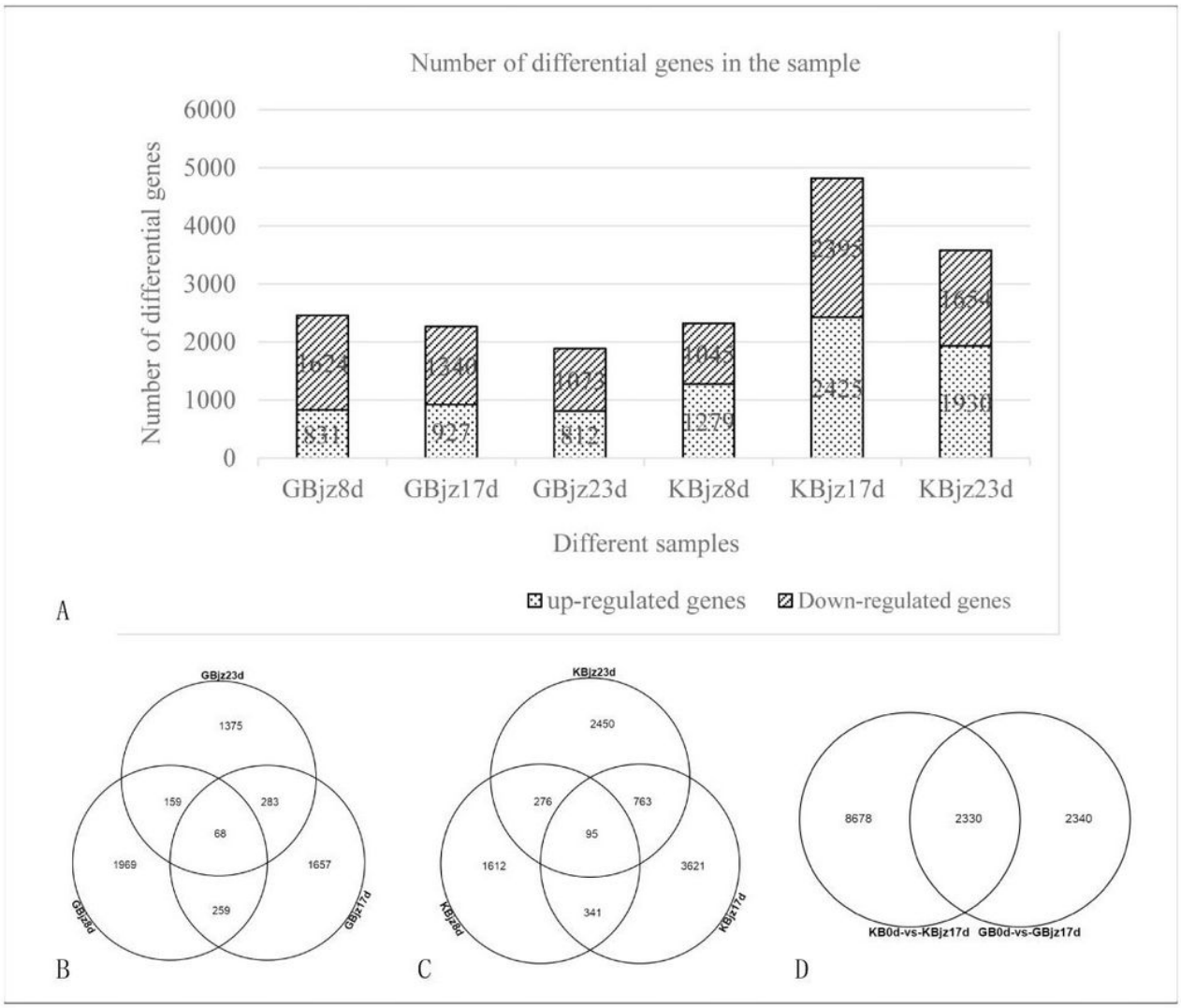

A: Quantity of DEGs in different samples

B: Venn diagrams of 283×anti-10 at different time point

C: Venn diagrams of Yuesang C44 at different time point

D: Venn diagrams of 283×anti-10 and Yuesang C44 comparison results at 17 days after inoculation

Figure 2

Summary images filtered by DEGs

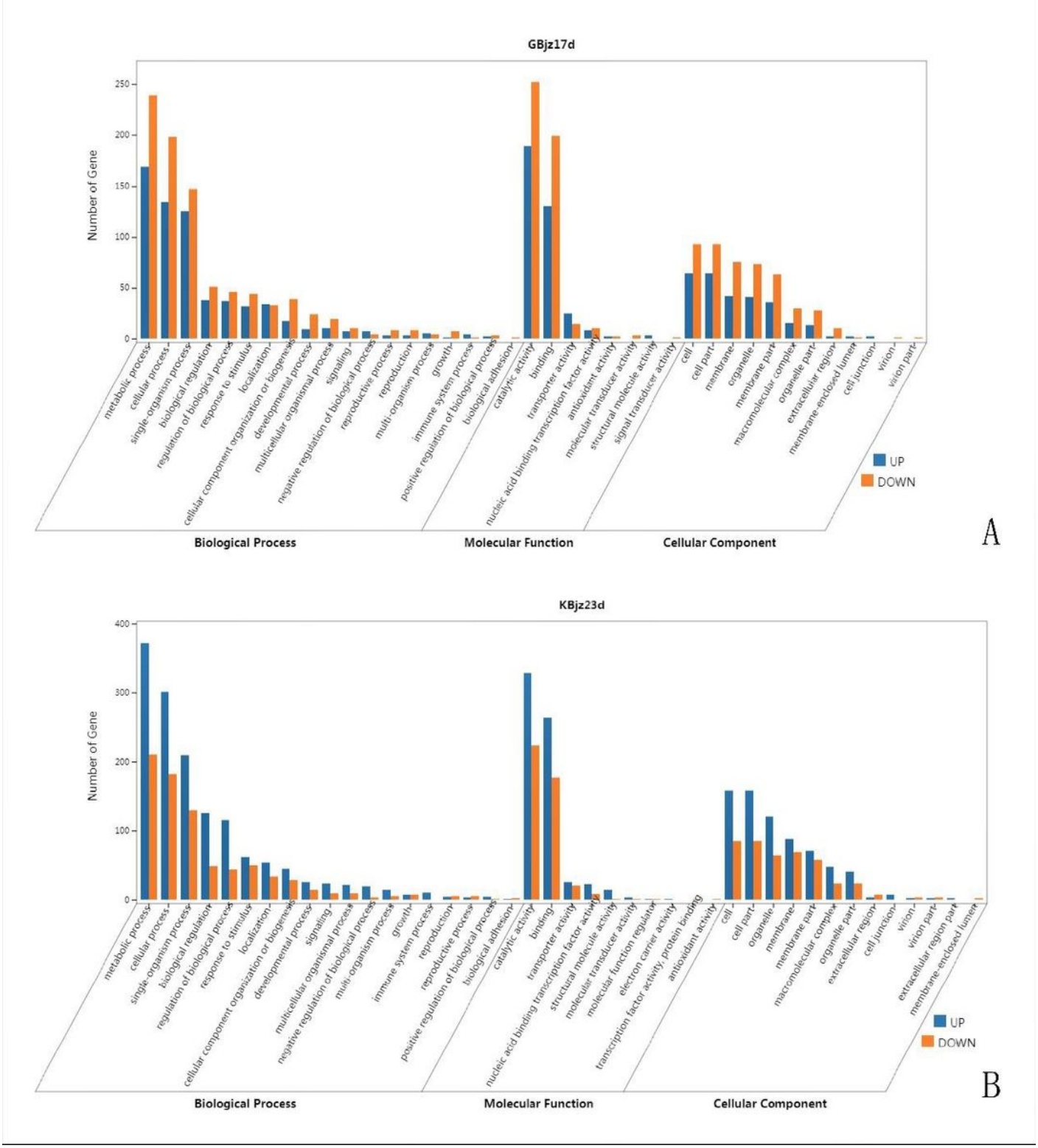

Figure 3

Fig. 3 GO Classification of DEGs in GBjz17d(A) and KBjz23d (B)

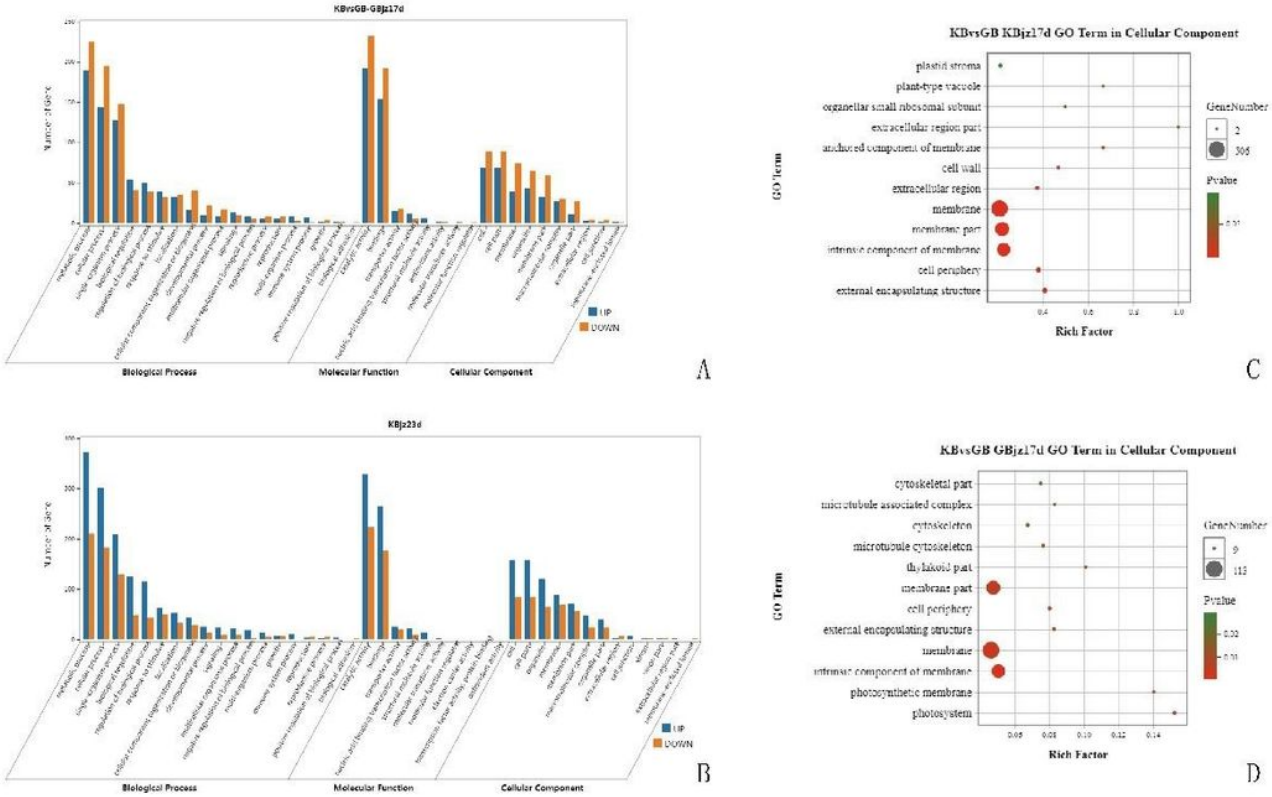

A: GO Classification of DEGs in GBjz17d

B: GO Classification of DEGs in KBjz23d

C: GO enrichment results of DEGs in KBjz23d

D: GO enrichment results of DEGs in GBjz17d

Figure 4

GO Classification and GO enrichment results of DEGs in KBvsGB KBjz17d and KBvsGB-GBjz1 7d

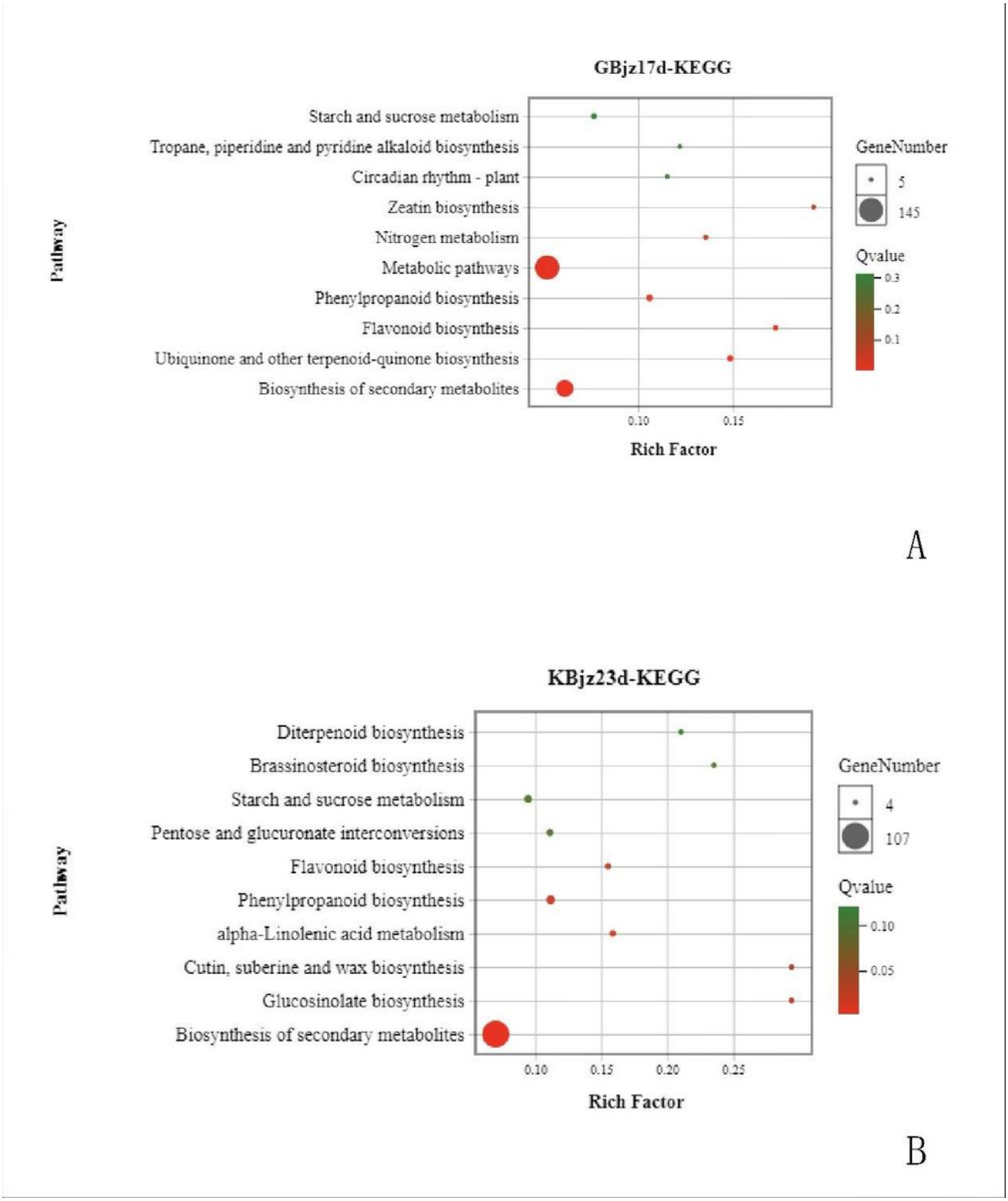

Figure 5

Fig. 5 Pathway enrichment results of DEGs in GBjz17d(and KBjz23d (B)

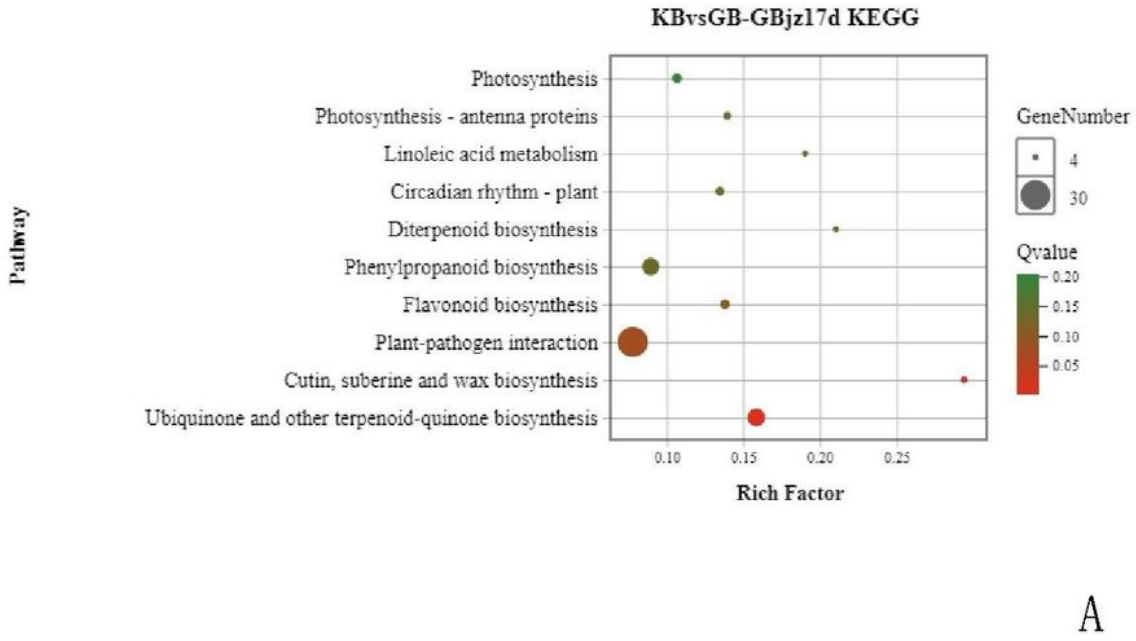

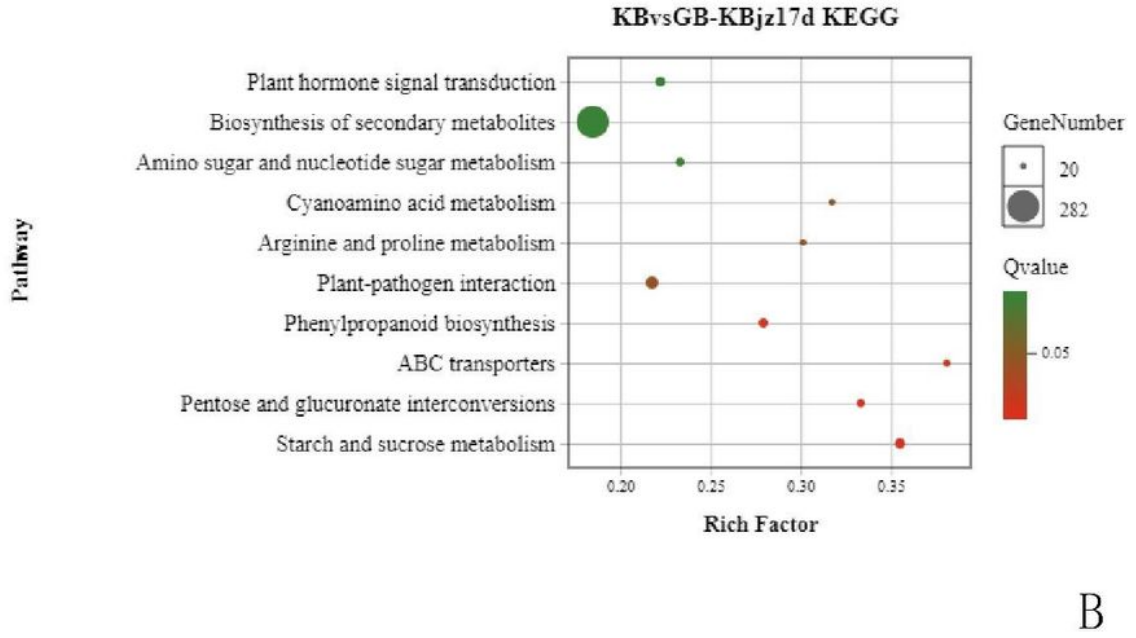

Figure 6

Pathway enrichment results of DEGs in comparison with 283×anti 10 (A) and Yuesang C44(B)

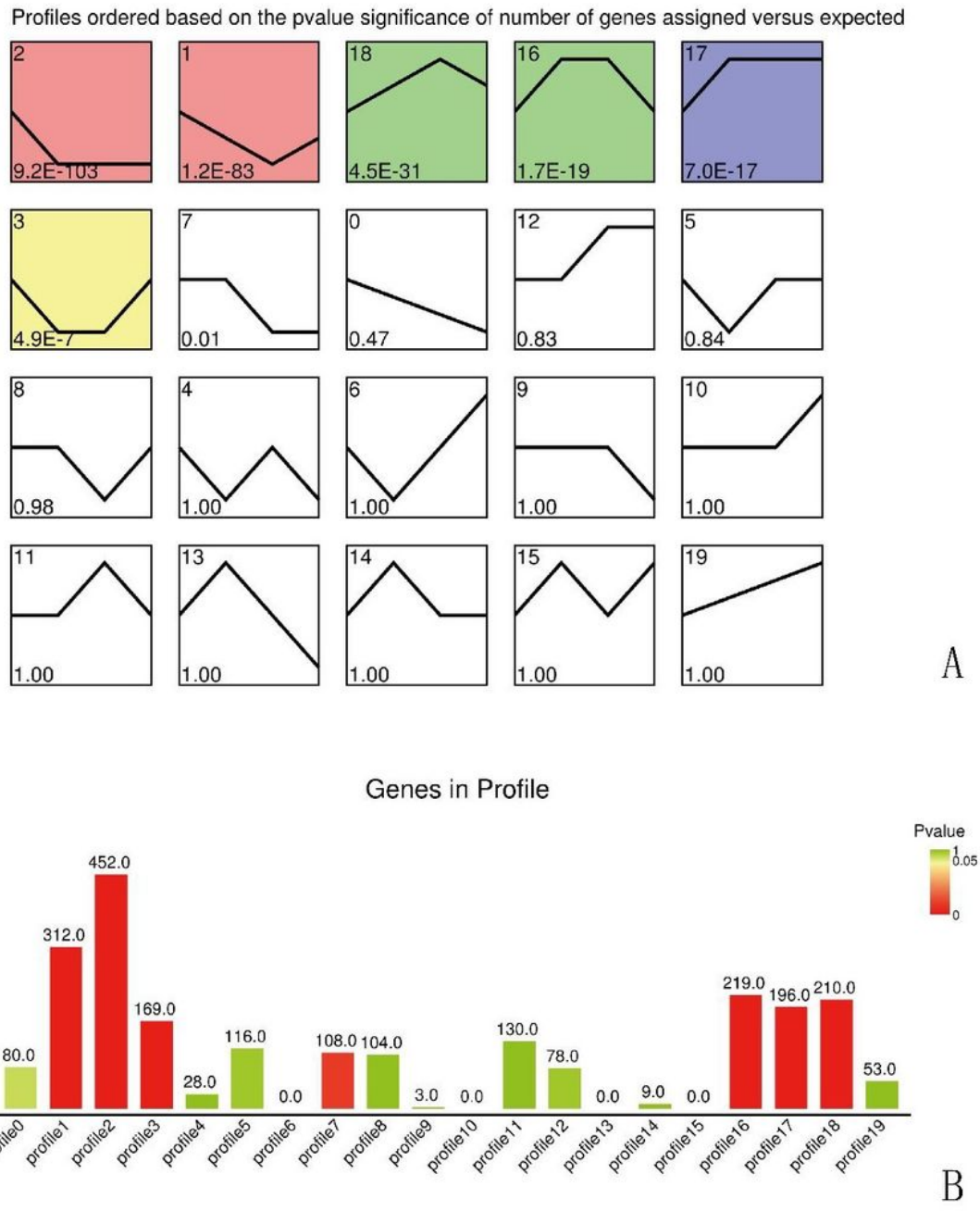

The lower left corner of the trend block is the P-value value. The value is the smaller, the stronger is the enrichment (as the same below).

Figure 7

Trends in DEGs of GBjz17d (A) and the number of genes for each profile (B)

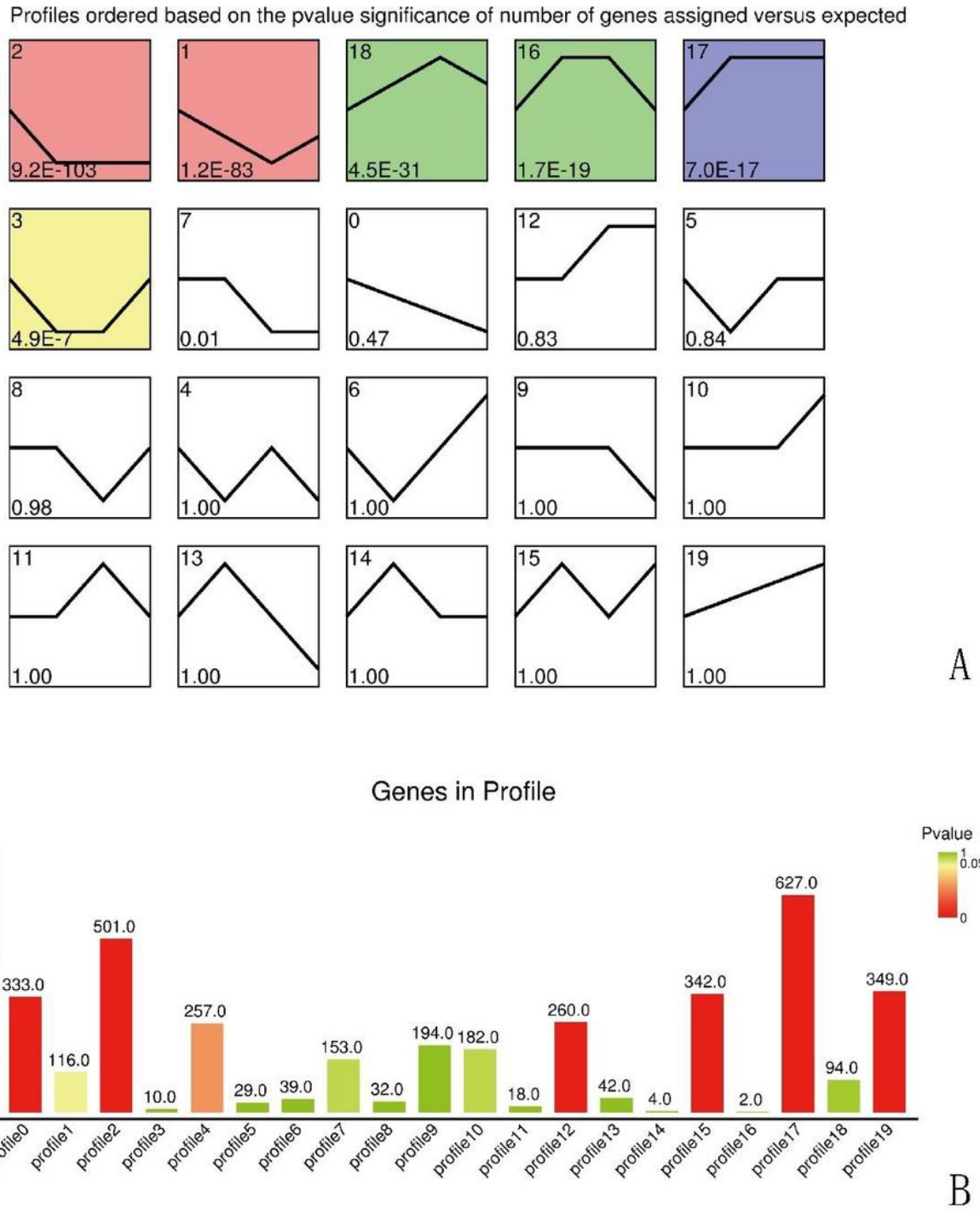

Figure 8

Trends in DEGs of KBjz23d (A) and the number of genes for each profile (B)

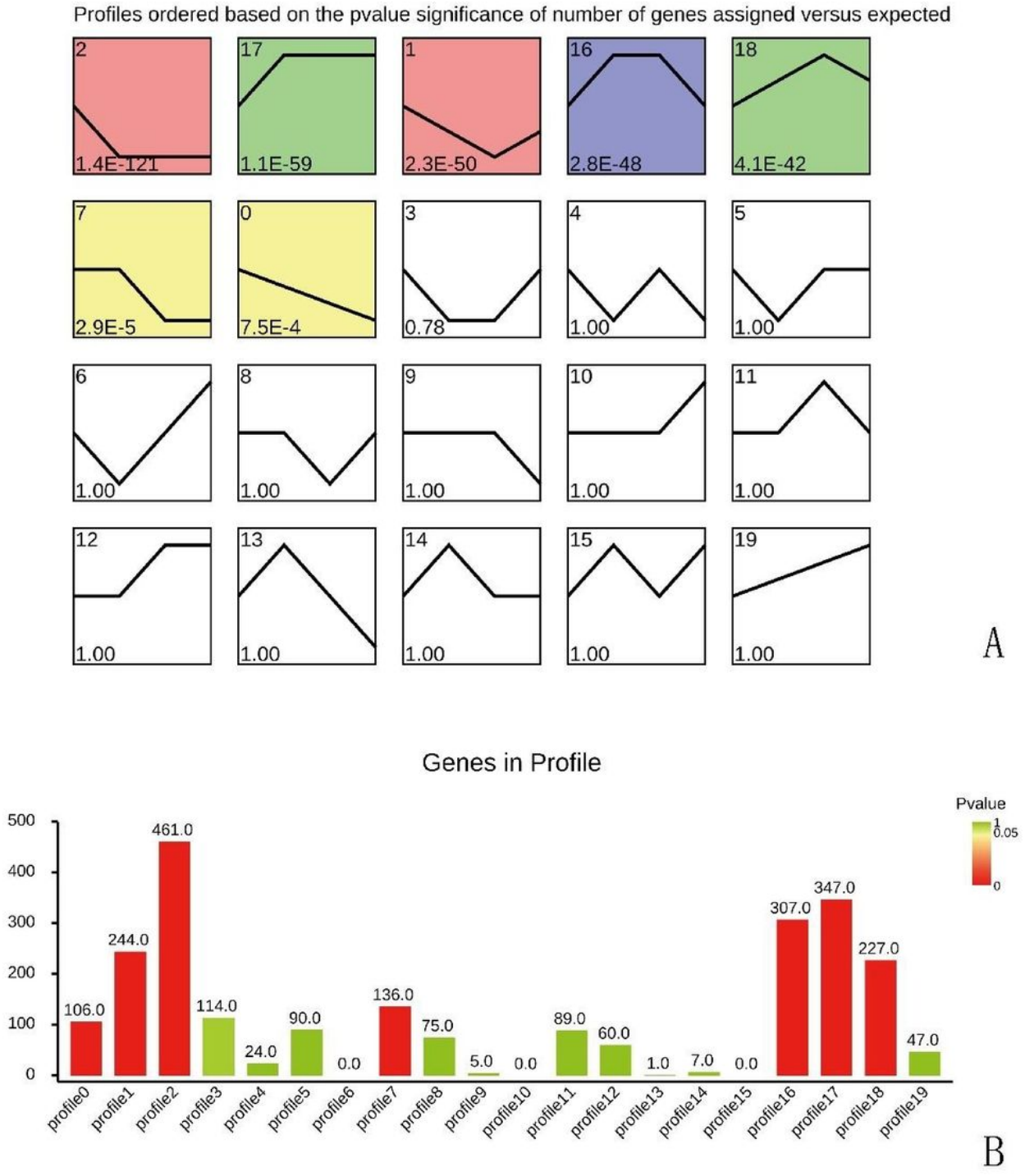

Figure 9

Trends in DEGs of KBvsGB GBjz17d (A) and the number of genes for each profile (B)

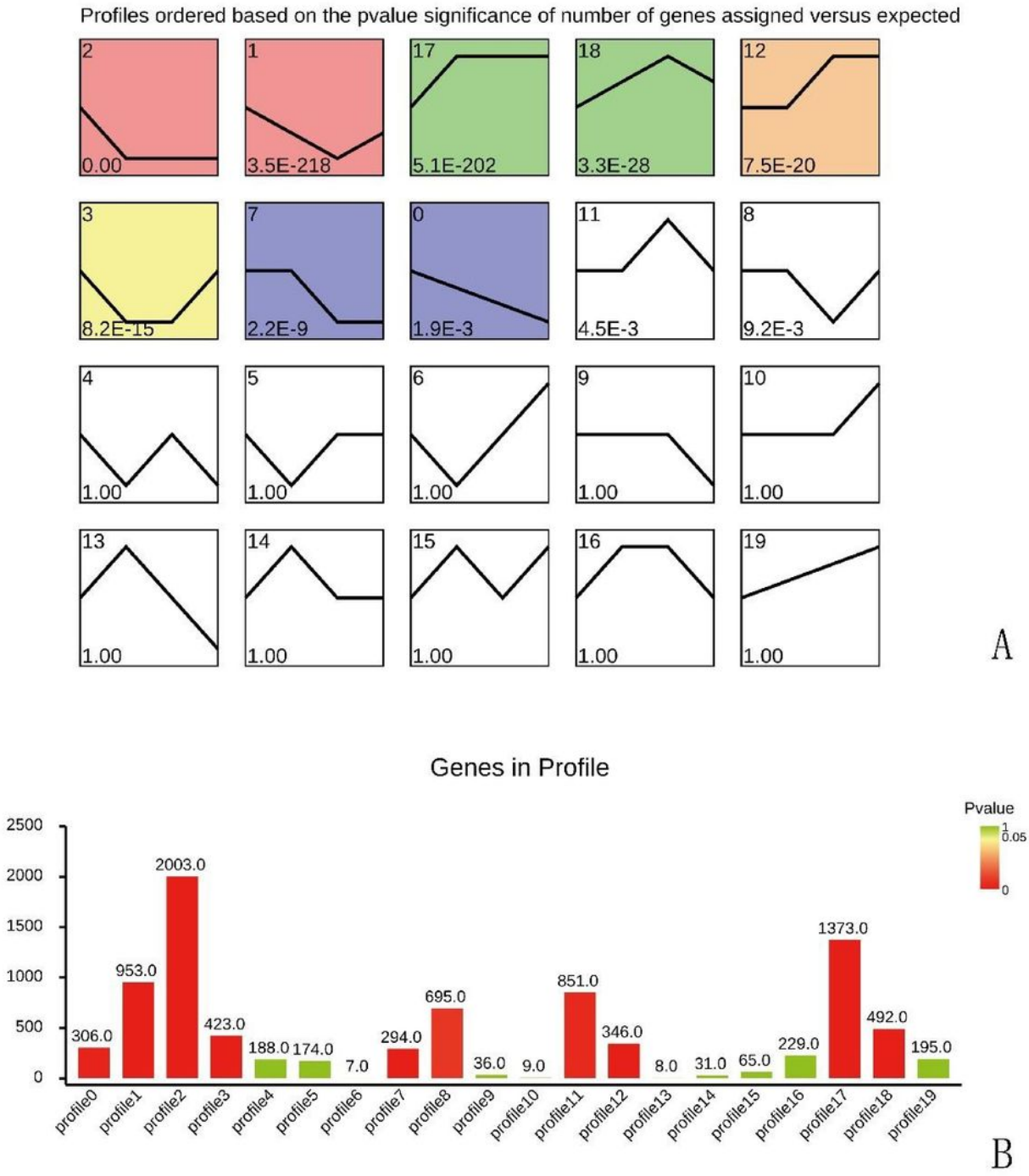

Figure 10

Trends in DEGs of KBvsGBKBjz17d (A) and the number of genes for each profile (B)

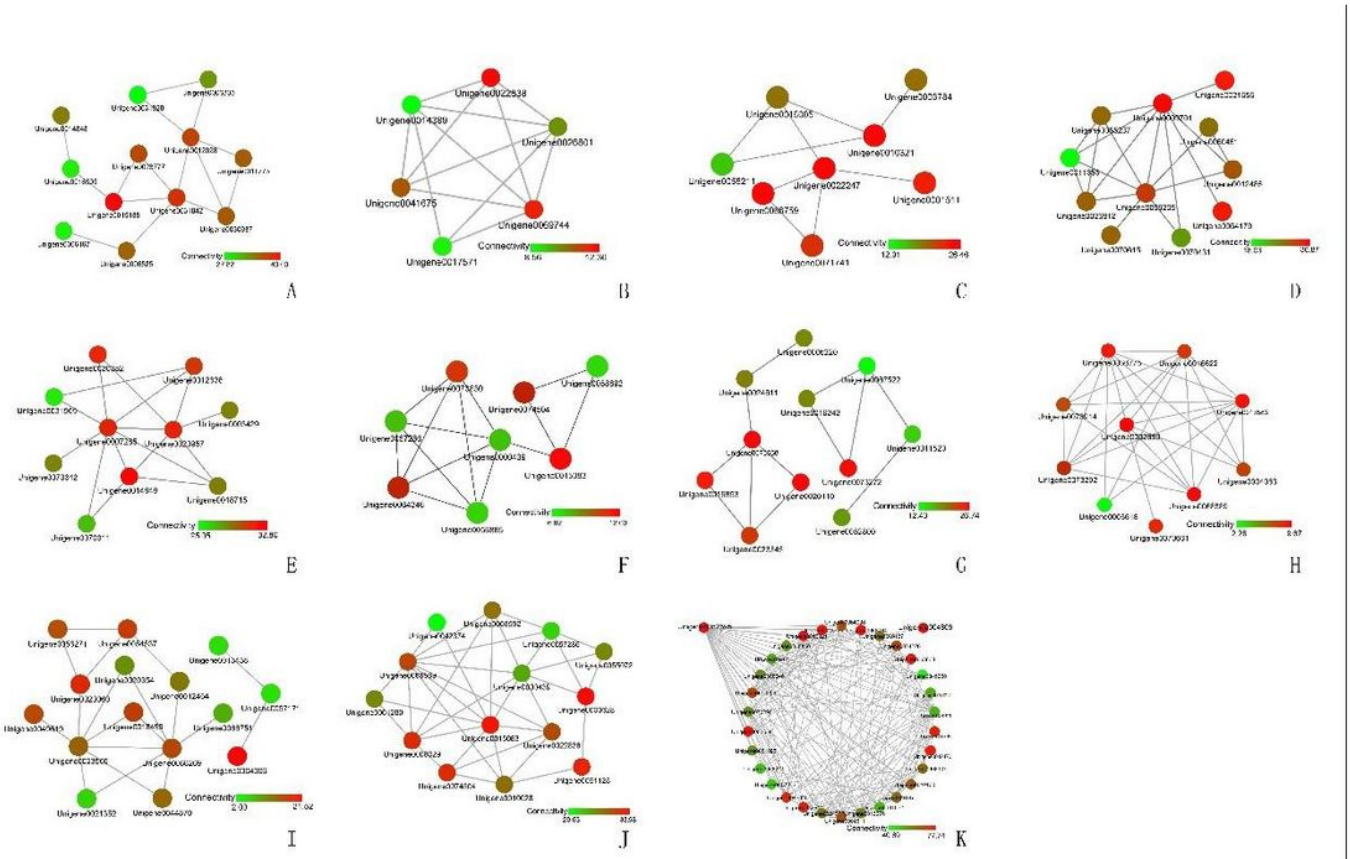

A: GBjz17d profile1 B: GBjz17d profile3 C: GBjz17d profile16 D: GBjz17d profile18
E: KBjz23d profile0 F: KBjz23d profile12 G: KBjz23d profile15 H: KBjz23d profile19
I: KBvsGB-KBjz17d profile3 J: KBvsGB-KBjz17d profile12 K: key trend of KBvsGB-GBjz17d

Figure 11

Co expression network analysis diagram of key trends

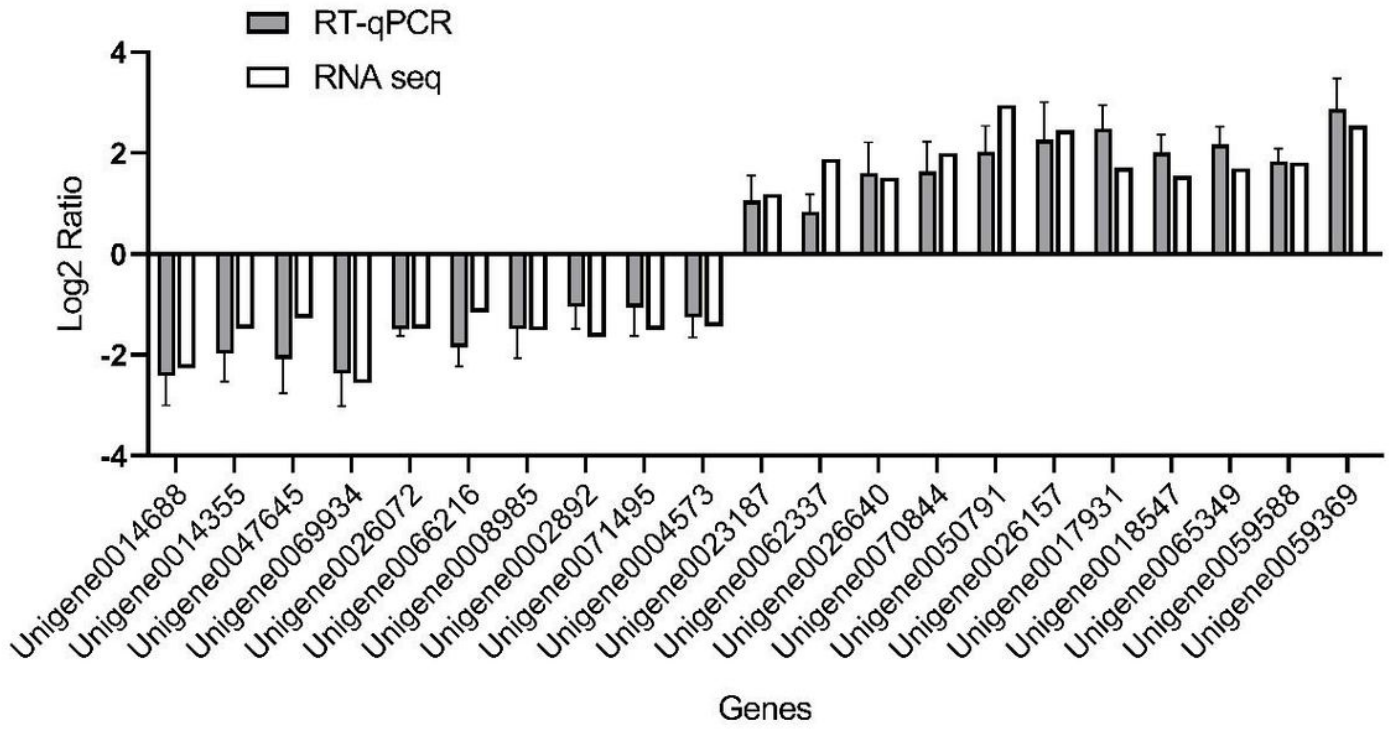

Figure 12

Validation results of DEGs by RT qPCR